A

Protocol	MethylEasy	Imprint	BisulFast	BisulFast Modified
Denaturation	Alkaline	Heat	Alkaline	Heat
Mass yields	79%	56%	72%	67%

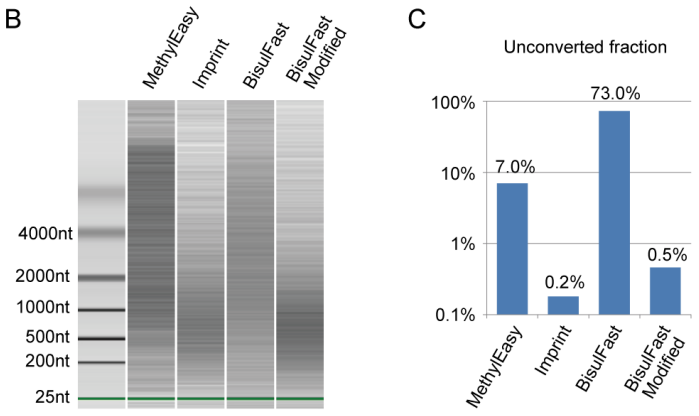

Supplementary Figure S1. Effect of DNA denaturation procedure on the efficiency of bisulfite conversion.

(A) Yield of DNA in bisulfite conversion. We used "MethylEasy" Xceed Rapid DNA Bisulphite Modification Kit (Human Genetic Signatures), "Imprint" bisulfite DNA modification kit (Sigma) and "BisulFast" DNA modification kit (Toyobo) according to the manufacturer's instructions. For the protocol indicated as "BisulFast, Modified", we omitted the alkaline denaturation step and instead denatured the genomic DNA dissolved in bisulfite salt solution by heating at 99 ºC for 6 min. "Alkaline" and "Heat" indicate the denaturation procedure used. "Mass yields" indicates the amount of obtained DNA, concentration of which was fluorometrically determined using Qubit ssDNA Assay Kit (Invitrogen) and Qubit fluorometer (Invitrogen), according to the manufacturer's instruction.

(B) Size distribution of bisulfite-treated DNA. DNAs subjected to heat denaturation were much more prominently fragmented than those subjected to alkaline denaturation. Electrophoresis was performed on Bioanalyzer 2100 (Agilent) using RNA 6000 pico kit (Agilent).

(C) PCR quantification of a region extremely refractory to bisulfite conversion. During the development of PBAT method, we noticed that several regions in the *A. thaliana* chloroplast genome appear to be highly methylated. Since the chloroplast DNA is known to escape methylation, it is likely that these regions are exceptionally refractory to bisulfite conversion. We thus used one of them as a model to identify conditions for efficient conversion. Primers used for qPCR to amplify the unconverted fragment were 5′-CCC CAT AGG CTT TCG CTT TCG CGT CTC TCT-3′ and 5′-TAG AGA ATT TGT GCG CTT GGG AGT CCC TGA-3′. We used serially diluted, untreated genomic DNA as a standard to determine the amount of unconverted DNA. These results indicated that heat denaturation results in slightly lower DNA recovery and much higher conversion rate than those with alkaline denaturation, presumably because the former induces much more prominent DNA fragmentation than the latter, thereby facilitating efficient denaturation and conversion.

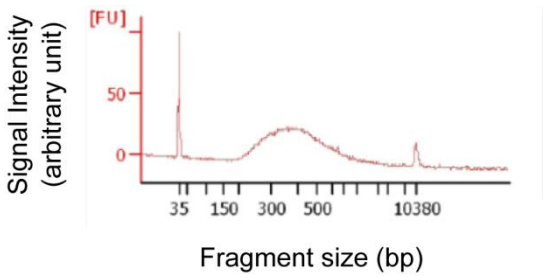

Supplementary Figure S2. Typical size distribution of template DNA prepared by the PBAT method.
Sequencing template DNA after the size fractionation with AMPure SPRI beads (see Materials and Methods) was electrophoresed by Bioanalyzer 2100 (Agilent)with High Sensitivity DNA Kit (Agilent). As intended, DNAs smaller than 200 bp were effectively removed.

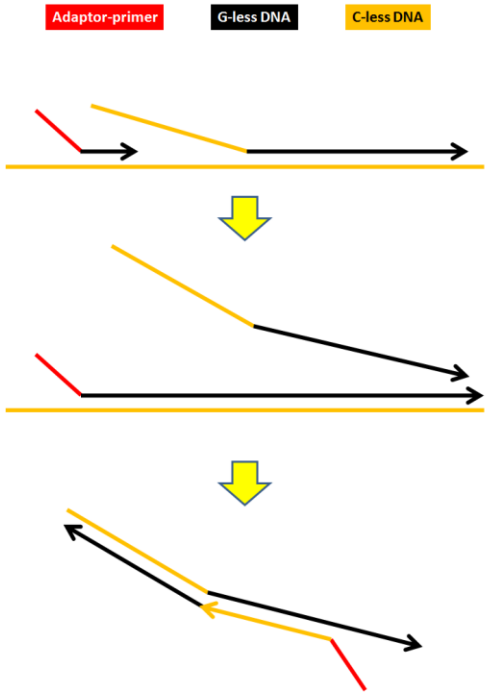

Supplementary Figure S3. A plausible mechanism to generate reads derived from the opposite strand.
Bisulfite treatment makes all the genomic DNA C-poor (colored in orange). During the first strand synthesis step in the PBAT method, not only the adaptor primer (red) but also the bisulfite-treated genomic DNA itself may prime the synthesis of complementary G-poor DNA (black) (*top*). If such a genomic DNA-primed strand is displaced by DNA polymerase extending another product (*middle*), then the displaced strand can serve as a template for the synthesis of C-poor DNA from the adaptor-primer (*bottom*), leading to reads derived from the unintended strand of genomic DNA occasionally found in the PBAT data.

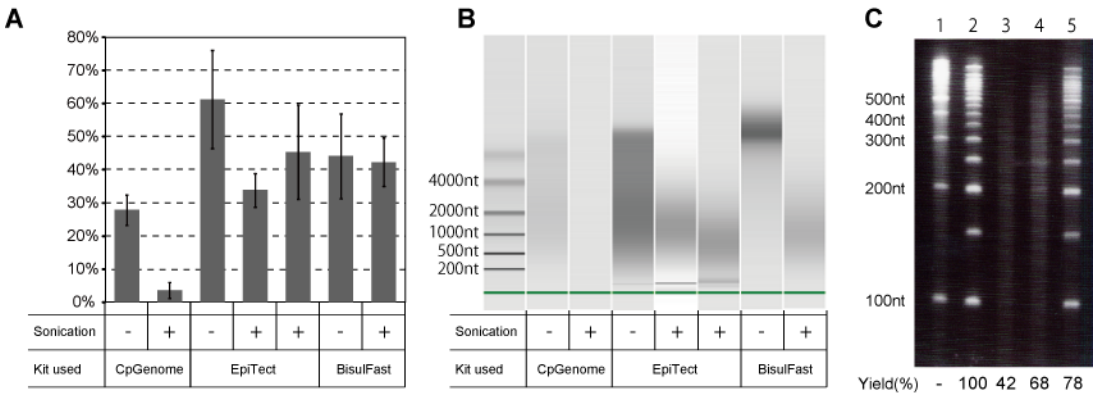

Supplementary Figure S4. Bisulfite-induced DNA loss and fragmentation.

(A) DNA loss by bisulfite treatment. Genomic DNA (100 ng) was bisulfite-treated and purified using 3 commercially available kits according to the manufacturers' instructions. To examine the effect of pre-fragmentation on DNA recovery, we prepared genomic DNA samples subjected to sonication-mediated fragmentation. For the bisulfite treatment of fragmented DNA using EpiTect, we tested both the standard protocol (*middle*) and the protocol for degraded DNA (*right*). Concentration of each DNA was fluorometrically determined using Quant-iT single stranded DNA Kit (Life technologies) and Qubit fluorometer (Invitrogen). Note that pre-fragmentation tends to reduce the yield of DNA.

(B) Size distribution of bisulfite-treated DNA. Samples quantified as above were electrophoresed by Bioanalyzer 2100 (Agilent) with RNA 6000 Pico RNA kit (Agilent).

(C) Bisulfite-induced DNA fragmentation. A DNA size standard (50-bp ladder, NEB) was bisulfite-treated, fluorometrically quantified and electrophoresed on a denaturing 6% polyacrylamide gel. Lane 1; 100-bp ladder (Bioneer), lane 2; input 50-bp ladder, lane 3; 50-bp ladder subjected to heat denaturation followed by bisulfite treatment and on-column desulfonation, lane 4; 50-bp ladder subjected to alkaline denaturation followed by bisulfite-treatment and on-column desulfonation, lane 5; 50-bp ladder subjected only to denaturation and mock on-column desulfonation. Note that heat denaturation led to more prominent DNA fragmentation than alkaline denaturation (see also Supplementary Figure S1).

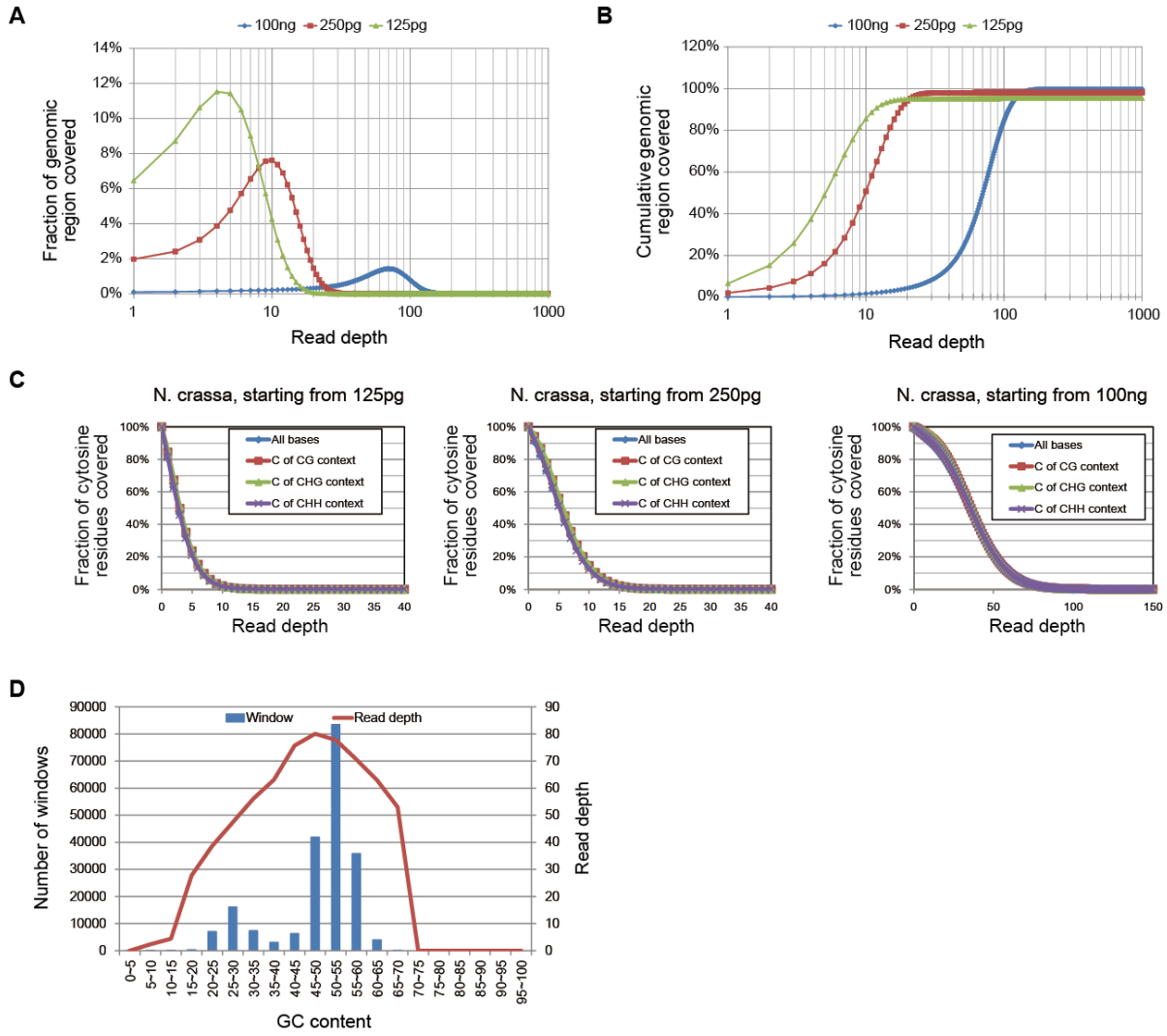

Supplementary Figure S5. *N. crassa* methylome determined by PBAT.

(A) Coverage of the *N. crassa* genome. The percent of the genome covered at the indicated read depth is shown for the PBAT data obtained from 100 ng, 250 pg and 125 pg of input DNA (Supplementary Table S1). Note that 6.5% of the templates generated from 100 ng of DNA (*i.e.*, equivalent to 6.5 ng of input DNA) was used for sequencing, whereas all the templates generated from 250 pg and 125 pg of DNA were sequenced.

(B) Cumulative coverage of the *N. crassa* genome. The percent of the genome covered by differing maximum depth of reads is shown for the three datasets.

(C) Strand-specific base coverage. The percent of all bases and cytosine residues in the indicated context covered by differing minimum number of reads is shown for the three datasets.

(D) GC content and median read depth were calculated for each of the 1,000-bp moving window with a step size of 200 bp in the genome. The bar and line plot indicate the number and relative read depth of windows with indicated GC content of the original genome sequence, respectively.

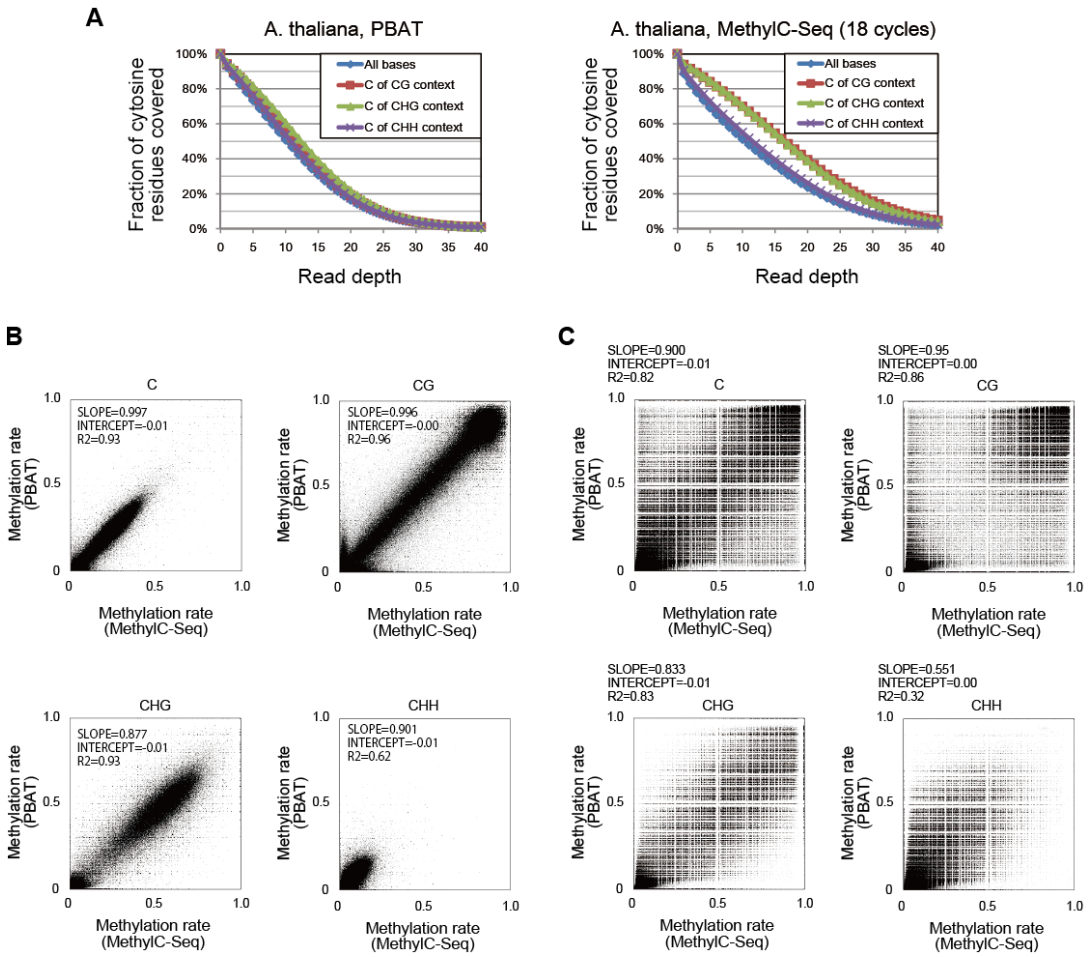

Supplementary Figure S6. Comparison of PBAT and MethylC-Seq data on the *A. thaliana* methylome.

(A) Strand-specific base coverage. The percent of all bases and cytosine residues in the indicated context covered by differing minimum number of reads is shown for the PBAT and MethylC-Seq data (Supplementary Table S2).

(B) The moving averages (window size, 1000 bp; step size, 200 bp) of methylation rate in the indicated sequence context were calculated from the PBAT and MethylC-Seq data and plotted for comparison.

(C) Methylation rate of each cytosine residue in the indicated sequence context was calculated from the two datasets and plotted for comparison. Note that the single nucleotide-level analysis is much more sensitive to fluctuation of the data, especially for the residues with lower coverage, than the window-based analysis, because the latter takes the average of all C residues in the window to buffer the effect of fluctuation. Thus, the single nucleotide level analysis inevitably leads to much wider scatter around the diagonal than the window-based analysis.

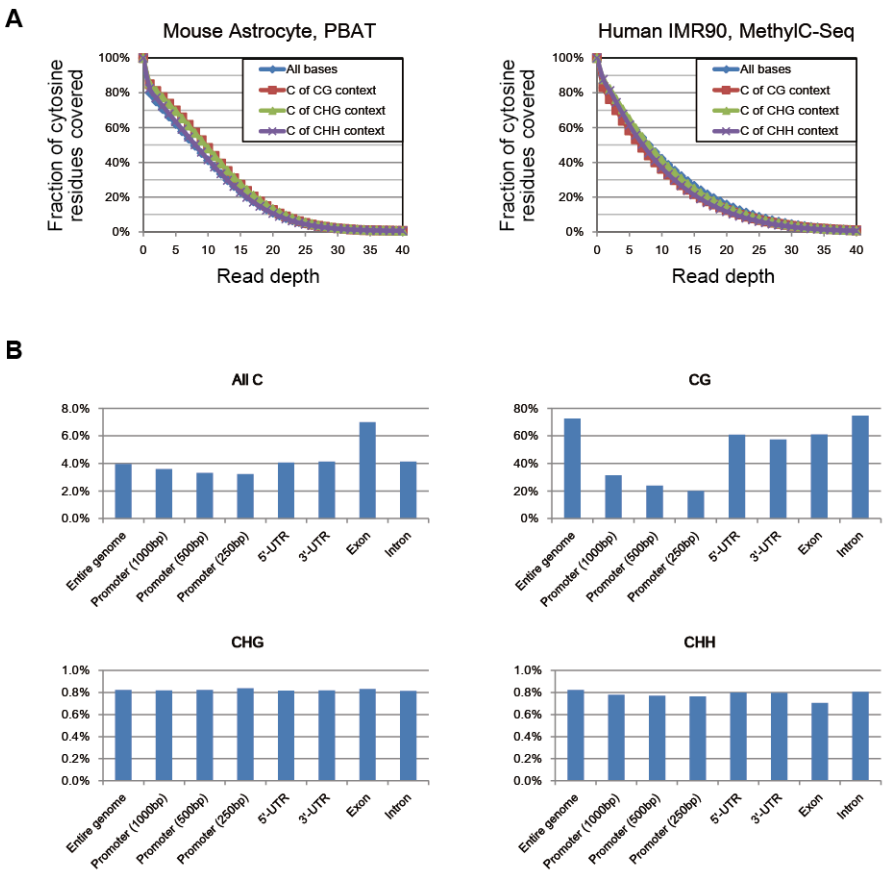

Supplementary Figure S7. Mouse astrocyte methylome determined by PBAT.

(A) Strand-specific base coverage. The percent of all bases and cytosine residues in the indicated context covered by differing minimum number of reads is shown for the mouse PBAT and human MethylC-Seq datasets (Supplementary Table S3).

(B) Methylation levels at the entire mouse genome and annotated genomic loci. Promoters were defined as 1000, 500 and 250 bp region upstream of transcriptional start sites. UTR; untranslated region.

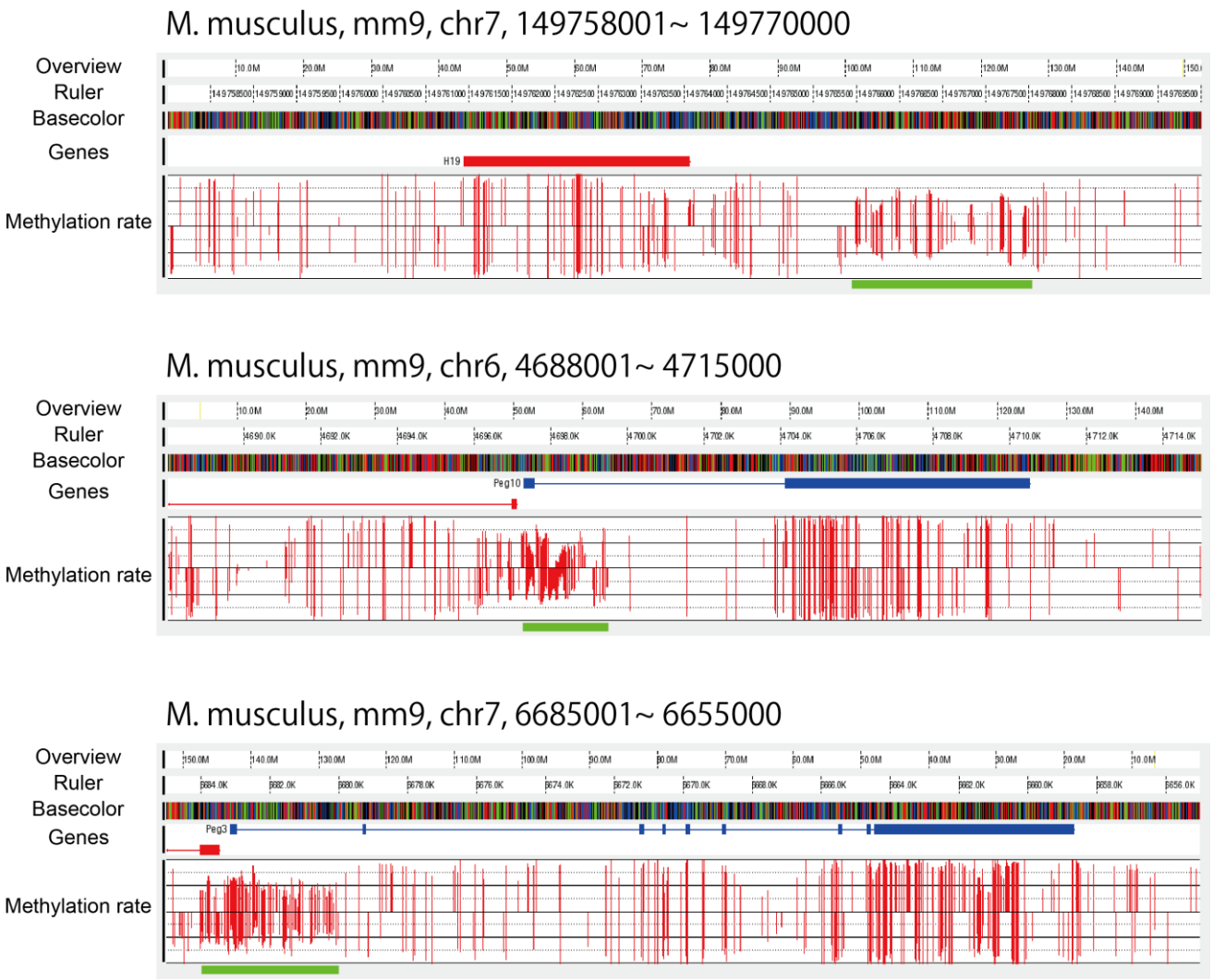

Supplementary Figure S8. Methylation status of mouse imprinted DMRs.

Browser shots were taken for the imprinted genes *H19*, *Peg10* and *Peg3*. Imprinted DMRs indicated by the green bars (23) showed ~50% methylation levels as expected, whereas other regions generally did higher methylation levels.

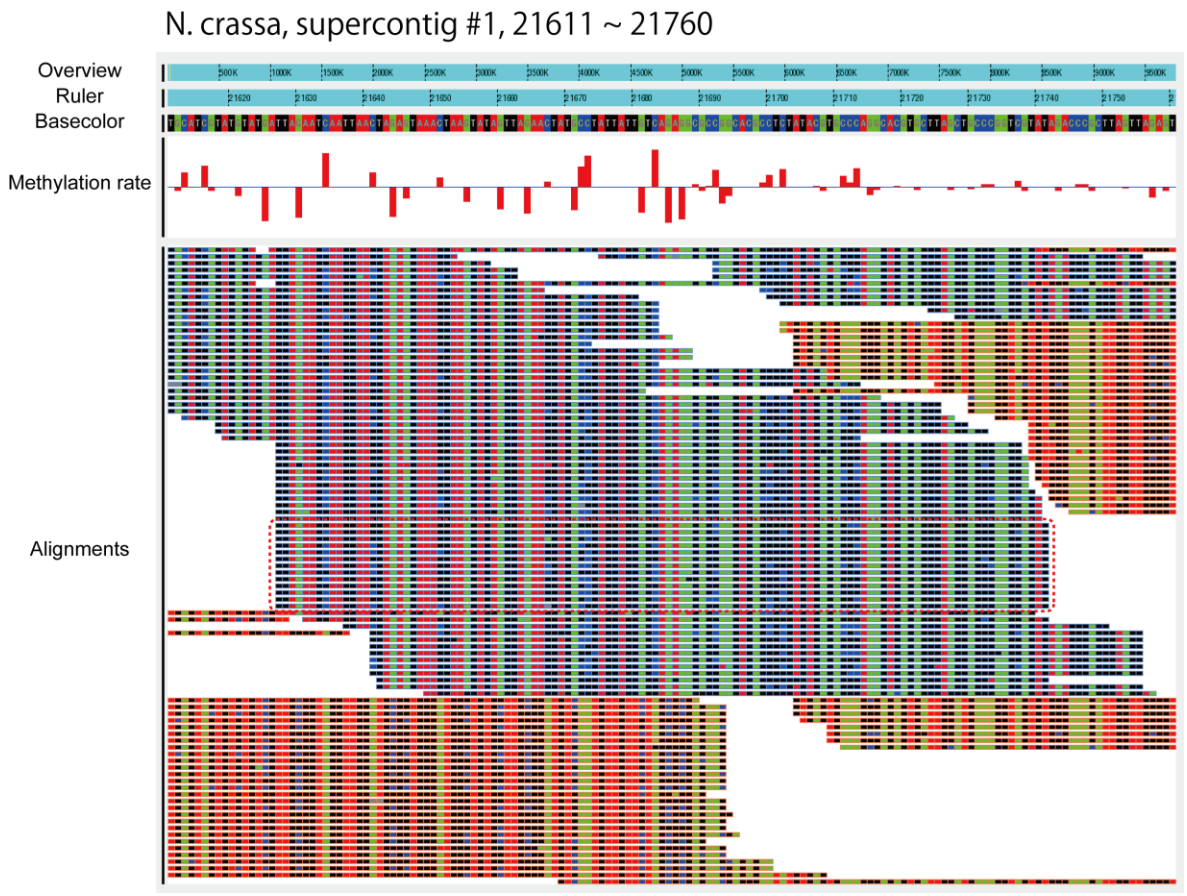

Supplementary Figure S9. An example of piled-up reads.

A browser shot was shown for an example of piled-up reads from the *N. crassa* data. The browser contained 5 tracks for overview, ruler, basecolor (nucleotide sequence), methylation rate and alignment. For the alignment track, reads mapped on top and bottom strands were shown as horizontal bars with blue and orange backgrounds, respectively. For both basecolor and alignment tracks, red, blue, green and black indicated A, C, G and T, respectively. The red dotted rounded rectangle indicated 13 piled-up reads. Notably, each of these 13 reads had a unique methylation pattern, indicating that these reads were all derived from independent DNA molecules and thus informative in estimating DNA methylation level.

A

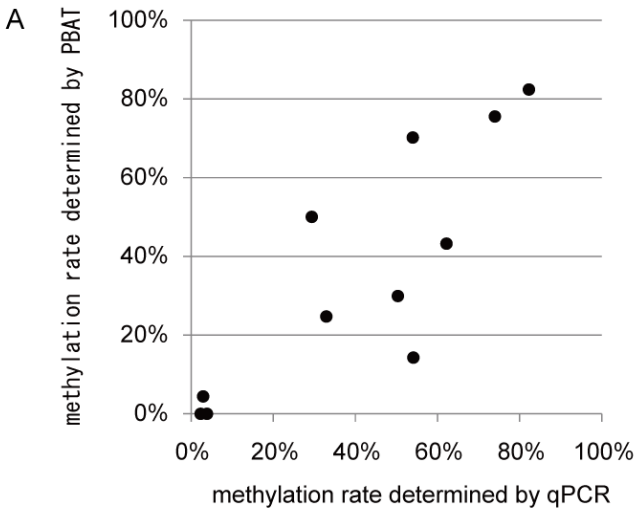

B

forward primer	reverse primer	methylation rate determined by qPCR	methylation rate determined by PBAT
GAGTGATAATAAAAAGGAAGGGTAGACGG	CTTTTACTACCACTACATTACTCCCCG	54%	14%
AATTGGCGTATTCTCGAAGGG	TTCCTTAATGCCTGAGCCAC	82%	82%
TAATTATTAAAGCCGCCGTACGAAG	AACGGCGGGTACTTTTATCGAG	74%	76%
TTGCTTCTCCCTTACTTGAGCTT	TGACCAACTTTCCTGCATCTAGTG	3%	4%
TTTTGTGTCGAACTAGGCGTAGG	TGTAATTTTTCTGGTACTGTTTCCCTC	2%	0%
TGTCAAGCTGAAAATTAAGGGGAG	AAAAACACCAAAAAACAACGTTCTAGAC	4%	0%
ACTACTAAATGAACGTTACTTCCGCAAAGA	ATAAATTACGCGCGGGACCTTTATTAGT	33%	25%
ATTGAAGATTCTAAAGAGGAAGAGGCTATC	TGCGGTTTCTTTTATAATTAATATTTCTCC	62%	43%
TGGTAGAAGACTTCATTAAAGCAGATAAGGA	GTTAATTAAATACCAGCCGGGCTTTCTAAG	29%	50%
GAATCTAAAAGGGCGTACAAATAAAGGATT	CCCGCTACTATACTATTGGACTAATTCTACGA	50%	30%
AACCTTATTAGTCTAAGGGAGGCTCCTAAT	CGCTGGATTTATATATTCTCGTGTATTTAGC	54%	70%

Supplementary Figure S10. Validation of methylation levels estimated by the PBAT data.

(A) Correlation between the methylation levels estimated from the PBAT and qPCR data (R = 0.84). We selected 11 GATC sites from the *Neurospora* genome and compared their methylation levels estimated by the PBAT data with those determined by a methylation-sensitive restriction enzyme-mediated qPCR assay. For the latter assay, the same genomic DNA used for PBAT was digested with BfuCI (NEB), which cuts GATC if the C is not methylated, and used as a template for qPCR amplification of the 11 sites. We quantified the amount of DNA refractory to BfuCI digestion using serially diluted intact genomic DNAs as a standard. We confirmed that all the 11 sites can be digested with >99% efficiency by MboI, a methylation-insensitive isoschizomer of BfuCI.

(B) Primer sequences used for the qPCR of the 11 GATC sites and the methylation levels estimated by the two methods.

Supplementary Table S1. Summary of PBAT method on *Neurospora crassa*

A. Mapping Summary

Method	Amount of starting DNA	Global amplification		Number of reads			
			Data source	Total	Uniquely mapped	Multiply mapped	Unmapped
PBAT	100 ng	no	DDBJ DRX000759 (116-nt single-end reads)	47,126,874 (100%)	27,880,723 (59.2%)	1,179,036 (2.5%)	18,067,115 (38.3%)
PBAT	250 pg	no	DDBJ DRX000760 (116-nt single-end reads)	7,218,087 (100%)	4,038,843 (56.0%)	188,458 (2.6%)	2,990,786 (41.4%)
PBAT	125 pg	no	DDBJ DRX000761 (116-nt single-end reads)	5,338,759 (100%)	2,194,304 (41.1%)	127,582 (2.4%)	3,016,873 (56.5%)

B. PBAT, *N. crassa* , starting from 100 ng DNA

	Target region (nt)	Mapped region (nt)	% coverage	Read amount (nt)	Fold-coverage
supercont10.1	9,798,893	9,781,379	99.8%	712,186,061	72.7x
supercont10.2	4,478,683	4,465,945	99.7%	313,524,054	70.0x
supercont10.3	5,274,802	5,260,804	99.7%	378,140,045	71.7x
supercont10.4	6,000,761	5,988,989	99.8%	424,175,265	70.7x
supercont10.5	6,436,246	6,424,874	99.8%	464,494,872	72.2x
supercont10.6	4,218,384	4,208,723	99.8%	296,007,027	70.2x
supercont10.7	4,255,303	4,243,442	99.7%	297,661,272	70.0x
supercont10.8~10.20	574,466	565,223	98.4%	95,272,576	165.8x
supercont10.21	64,840	64,836	100.0%	42,324,056	652.7x
total	41,102,378	41,004,215	99.8%	3,023,785,228	73.6x

C. PBAT, *N. crassa* , starting from 250 pg DNA

	Target region (nt)	Mapped region (nt)	% coverage	Read amount (nt)	Fold-coverage
supercont10.1	9,798,893	9,643,500	98.4%	104,559,426	10.7x
supercont10.2	4,478,683	4,395,295	98.1%	46,430,594	10.4x
supercont10.3	5,274,802	5,187,064	98.3%	55,981,290	10.6x
supercont10.4	6,000,761	5,885,704	98.1%	62,389,747	10.4x
supercont10.5	6,436,246	6,337,448	98.5%	68,761,967	10.7x
supercont10.6	4,218,384	4,144,696	98.3%	44,020,521	10.4x
supercont10.7	4,255,303	4,162,441	97.8%	43,910,468	10.3x
supercont10.8~10.20	574,466	527,298	91.8%	13,697,912	23.8x
supercont10.21	64,840	64,786	99.9%	5,711,236	88.1x
total	41,102,378	40,348,232	98.2%	445,463,161	10.8x

D. PBAT, *N. crassa* , starting from 125 pg DNA

	Target region (nt)	Mapped region (nt)	% coverage	Read amount (nt)	Fold-coverage
supercont10.1	9,798,893	9,377,222	95.7%	56,712,925	5.8x
supercont10.2	4,478,683	4,265,067	95.2%	25,285,068	5.6x
supercont10.3	5,274,802	5,051,590	95.8%	30,124,795	5.7x
supercont10.4	6,000,761	5,710,953	95.2%	33,670,644	5.6x
supercont10.5	6,436,246	6,173,848	95.9%	37,159,647	5.8x
supercont10.6	4,218,384	4,022,675	95.4%	23,702,042	5.6x
supercont10.7	4,255,303	4,033,518	94.8%	23,766,532	5.6x
supercont10.8~10.20	574,466	475,662	82.8%	7,457,340	13.0x
supercont10.21	64,840	64,628	99.7%	3,056,827	47.1x
total	41,102,378	39,175,163	95.3%	240,935,820	5.9x

Supplementary Table S2. Comparison between MethylC-Seq and PBAT data for *Arabidopsis thaliana*

A. Mapping Summary

Method	Amount of starting DNA	Global amplification		[a]Number of reads			
			Data source	Total	Uniquely mapped	Multiply mapped	Unmapped
MethylC-Seq, 18 cycles of PCR amplification	5.0 µg	18 cycles of PCR	NCBI SRA SRX002495 (56-nt, single-end reads)	144,409,810 (100%)	64,368,550 (44.6%)	34,017,037 (23.6%)	46,024,223 (31.9%)
MethylC-Seq, 4cycles of PCR amplification[b]	2.0 µg	4 cycles of PCR	NCBI SRA SRX096408 (101-nt, single-end reads)	55,500,000 (100%)	33,226,080 (59.9%)	21,738,815 (39.2%)	535,105 (1.0%)
PBAT	0.1 µg	no	DDBJ DRX000762, DRX000763 (76- and 121-nt single-end reads)	78,490,558 (100%)	35,858,373 (45.7%)	21,065,230 (26.8%)	21,566,955 (27.5%)

[a]MethylC-Seq data and PBAT data were aligned to the reference genome using the same mapping method.

[b]To adjust depth of reads among three datasets, number of reads for this dataset is reduced appropriately.

B. MethylC-Seq data, 18 cycles of PCR amplification

	Target region (nt)	Mapped region (nt)	% coverage	Read amount (nt)	Fold-coverage
Chr1	30,432,563	28,185,315	92.6%	745,754,763	24.5x
Chr2	19,705,359	18,564,020	94.2%	506,702,890	25.7x
Chr3	23,470,805	22,240,386	94.8%	632,407,216	26.9x
Chr4	18,585,042	17,532,356	94.3%	482,623,520	26.0x
Chr5	26,992,728	25,340,318	93.9%	704,554,348	26.1x
subtotal	119,186,497	111,862,395	93.9%	3,072,042,737	25.8x
ChrC	154,478	153,325	99.3%	103,370,020	669.2x
ChrM	366,924	236,875	64.6%	47,131,394	128.5x
total	119,707,899	112,252,595	93.8%	3,222,544,151	26.9x

C. MethylC-Seq data, 4 cycles of PCR amplification

	Target region (nt)	Mapped region (nt)	% coverage	Read amount (nt)	Fold-coverage
Chr1	30,432,563	28,762,007	94.5%	680,259,131	22.4x
Chr2	19,705,359	19,000,346	96.4%	503,131,040	25.5x
Chr3	23,470,805	22,739,791	96.9%	615,619,374	26.2x
Chr4	18,585,042	17,971,162	96.7%	477,216,317	25.7x
Chr5	26,992,728	25,898,974	95.9%	666,745,499	24.7x
subtotal	119,186,497	114,372,280	96.0%	2,942,971,361	24.7x
ChrC	154,478	152,542	98.7%	332,278,909	2151.0x
ChrM	366,924	192,065	52.3%	27,567,979	75.1x
total	119,707,899	114,716,887	95.8%	3,302,818,249	27.6x

D. PBAT data

	Target region (nt)	Mapped region (nt)	% coverage	Read amount (nt)	Fold-coverage
Chr1	30,432,563	28,964,599	95.2%	677,020,538	22.2x
Chr2	19,705,359	19,154,222	97.2%	494,748,707	25.1x
Chr3	23,470,805	22,857,598	97.4%	579,509,137	24.7x
Chr4	18,585,042	18,085,050	97.3%	455,923,222	24.5x
Chr5	26,992,728	26,060,744	96.5%	640,243,634	23.7x
subtotal	119,186,497	115,122,213	96.6%	2,847,445,238	23.9x
ChrC	154,478	154,236	99.8%	434,947,984	2815.6x
ChrM	366,924	252,398	68.8%	140,215,255	382.1x
total	119,707,899	115,528,847	96.5%	3,422,608,477	28.6x

Supplementary Table S3. Mapping summary of mouse astrocyte and human IMR90 cell

A. Mapping Summary

Method	Sample	Amount of starting DNA	Global amplification	Data source	[a]Number of reads			
					Total	Uniquely mapped	Multiply mapped	Unmapped
PBAT	Mouse, astrocyte	0.1 µg	no	DDBJ DRX001198 (121-nt, single-end reads)	948,882,874 (100%)	614,791,432 (64.8%)	52,652,359 (5.5%)	281,439,083 (29.7%)
MethylC-Seq	Human, IMR90 cell	5.0 µg	4 cycles of PCR	NCBI SRA SRX006783 (84-nt, single-end reads)	1,335,097,975 (100%)	895,279,997 (67.1%)	66,343,995 (5.0%)	373,473,983 (28.0%)

[a]PBAT and MethylC-Seq data were aligned to the reference genomes for mouse and human or mm9 and hg19 downloaded from UCSC, respectively, using the same mapping method.

B. PBAT, Mouse astrocyte

	Target region (nt)	Mapped region (nt)	% coverage	Read amount (nt)	Fold-coverage
chr1	197,195,432	177,982,244	90.3%	3,945,712,558	20.0x
chr2	181,748,087	166,010,489	91.3%	6,564,637,897	36.1x
chr3	159,599,783	144,374,386	90.5%	3,124,371,147	19.6x
chr4	155,630,120	138,954,705	89.3%	3,164,955,396	20.3x
chr5	152,537,259	136,150,979	89.3%	3,089,061,325	20.3x
chr6	149,517,037	135,760,827	90.8%	3,098,043,639	20.7x
chr7	152,524,553	126,469,768	82.9%	2,898,442,082	19.0x
chr8	131,738,871	116,622,223	88.5%	2,659,977,368	20.2x
chr9	124,076,172	113,910,380	91.8%	3,477,637,080	28.0x
chr10	129,993,255	118,095,985	90.8%	2,602,983,062	20.0x
chr11	121,843,856	113,098,603	92.8%	2,712,399,102	22.3x
chr12	121,257,530	107,671,949	88.8%	2,997,849,828	24.7x
chr13	120,284,312	108,070,795	89.8%	2,411,672,691	20.0x
chr14	125,194,864	108,220,582	86.4%	2,385,049,700	19.1x
chr15	103,494,974	93,972,710	90.8%	2,121,635,781	20.5x
chr16	98,319,150	88,651,768	90.2%	1,935,827,154	19.7x
chr17	95,272,651	85,375,315	89.6%	1,934,864,821	20.3x
chr18	90,772,031	81,953,300	90.3%	1,833,347,022	20.2x
chr19	61,342,430	55,110,221	89.8%	1,253,868,764	20.4x
chrX	166,650,296	134,522,710	80.7%	2,365,963,375	14.2x
chrY	15,902,555	1,684,888	10.6%	22,219,325	1.4x
others*	70,853,964	13,498,262	19.1%	994,577,371	14.0x
subtotal	2,725,749,182	2,366,163,089	86.8%	57,595,096,488	21.1x
chrM	16,299	16,299	100.0%	46,374,003	2845.2x
total	2,725,765,481	2,366,179,388	86.8%	57,641,470,491	21.1x

*chr1_random, chr3_random, chr4_random, chr5_random, chr7_random, chr8_random, chr9_random, chr13_random, chr16_random, chr17_random, chrX_random, chrY_random and chrUn_random.

Supplementary Table S3. Mapping summary of mouse astrocyte and human IMR90 cell (continued)

C. MethylC-Seq, Human IMR90 cell

	Target region (nt)	Mapped region (nt)	% coverage	Read amount (nt)	Fold-coverage
chr1	249,250,621	214,492,462	86.1%	5,162,028,181	20.7x
chr2	243,199,373	230,166,103	94.6%	5,568,334,321	22.9x
chr3	198,022,430	189,211,270	95.6%	4,533,363,804	22.9x
chr4	191,154,276	181,365,292	94.9%	4,434,910,420	23.2x
chr5	180,915,260	170,758,054	94.4%	4,077,307,358	22.5x
chr6	171,115,067	157,704,110	92.2%	3,878,772,331	22.7x
chr7	159,138,663	149,053,303	93.7%	3,569,533,183	22.4x
chr8	146,364,022	137,874,665	94.2%	3,296,570,468	22.5x
chr9	141,213,431	109,325,541	77.4%	2,499,210,030	17.7x
chr10	135,534,747	125,109,749	92.3%	3,236,651,159	23.9x
chr11	135,006,516	126,937,413	94.0%	3,001,739,805	22.2x
chr12	133,851,895	126,340,322	94.4%	3,000,790,537	22.4x
chr13	115,169,878	93,167,349	80.9%	2,203,538,300	19.1x
chr14	107,349,540	85,351,918	79.5%	1,998,010,411	18.6x
chr15	102,531,392	76,764,322	74.9%	1,767,485,898	17.2x
chr16	90,354,753	74,289,141	82.2%	1,750,961,698	19.4x
chr17	81,195,210	73,415,226	90.4%	1,585,974,217	19.5x
chr18	78,077,248	72,656,265	93.1%	1,806,048,752	23.1x
chr19	59,128,983	52,721,013	89.2%	1,161,204,857	19.6x
chr20	63,025,520	57,778,892	91.7%	1,320,105,083	20.9x
chr21	48,129,895	33,705,892	70.0%	849,501,886	17.7x
chr22	51,304,566	32,553,755	63.5%	643,874,248	12.6x
chrX	155,270,560	141,070,120	90.9%	3,225,440,674	20.8x
chrY	59,373,566	6,729,542	11.3%	134,466,236	2.3x
others*	41,467,281	4,874,679	11.8%	430,030,730	10.4x
subtotal	3,137,144,693	2,723,416,398	86.8%	65,135,854,587	20.8x
chrM	16,571	16,056	96.9%	59,483,414	3589.6x
total	3,137,161,264	2,723,432,454	86.8%	65,195,338,001	20.8x

*chr6_apd_hap1, chr6_cox_hap2, chr6_dbb_hap3, chr6_mcf_hap5, chr6_qbl_hap6, chr4_ctg9_hap1, chr6_mann_hap4, chr6_ssto_hap7, chrUn_gl000211~chrUn_gl000249, chr17_ctg5_hap1, chr1_gl000191_random, chr1_gl000192_random, chr4_gl000193_random, chr4_gl000194_random, chr7_gl000195_random, chr8_gl000196_random, chr8_gl000197_random, chr9_gl000198_random~chr9_gl000201_random, chr11_gl000202_random, chr17_gl000203_random~chr17_gl000206_random, chr18_gl000207_random, chr19_gl000208_random, chr19_gl000209_random and chr21_gl000210_random